ISSN: 2538-2152; ECOPERSIA 2026;14(2): 115-132.

Spatial Analysis of Future Land-Use Impacts on Carbon Sequestration and Priority Area Identification in the Kojur Watershed using Hotspot and Moran's I Techniques

ARTICLEINFO

Article Type
Original Research

Authors
Halime Joloro, *M.Sc.*[1]
Ghasem Ali Dianati Tilaki, *Ph.D.*[2]*
Hadi Memarian, *Ph.D.*[3]
Yahya Kooch, *Ph.D.*[4]

How to cite this article
Joloro H., Dianati Tilaki GH.A., Memarian H., Kooch Y. Spatial Analysis of Future Land-Use Impacts on Carbon Sequestration and Priority Area Identification in the Kojur Watershed using Hotspot and Moran's I Techniques. ECOPERSIA 2026;14(2): 115-132.

DOI:
10.48311/ecopersia.2026.116529.1004

[1] Ph.D. Student, Department of Rangeland Science and Engineering, Faculty of Natural Resources, Tarbiat Modares University, Noor, Mazandaran Province, Iran.
[2] Associate Professor, Department of Range Management, Faculty of Natural Resources, Tarbiat Modares University, Noor, Mazandaran Province, Iran.
[3] Associate Professor, Department of Watershed Management, Faculty of Natural Resources and Environment, University of Birjand, Birjand, South Khorasan Province, Iran.
[4] Associate Professor, Department of Range Management, Faculty of Natural Resources, Tarbiat Modares University, Noor, Mazandaran Province, Iran.

**** Correspondence***
Address: Department of Range Management, Faculty of Natural Resources, Tarbiat Modares University, Noor, Mazandaran Province, Iran.
Tel: +981144998000,
Email: dianatig@modares.ac.ir

Article History
Received: May 18, 2025
Accepted: Febraury 26, 2026
Published: Febraury 28, 2026

ABSTRACT

Aims: Land-use and land-cover (LULC) dynamics are central drivers of terrestrial Carbon fluxes. This study aimed to assess the spatial heterogeneity of Carbon storage in the Kojur Watershed and to determine how topographic factors influence Carbon sequestration across historical and projected timeframes.

Materials & Methods: LULC maps for 2003, 2013, and 2023 were generated using satellite imagery and the Land Change Modeler (LCM). Future scenarios for 2035 and 2050 were simulated using the Cellular Automata Markov (Ca-Markov) model under a business-as-usual assumption, which projected historical land-use transitions and socio-economic trends forward. The InVEST Carbon module estimated Carbon storage in four pools: aboveground biomass, belowground biomass, litter, and soil. Spatial clustering was analyzed using Moran's I and Getis-Ord Gi* statistics.

Findings: Carbon storage showed a consistent, statistically significant clustered pattern across all years. Forests held the most Carbon (≈2.5-2.6 million tons), rangelands moderate (≈1.2-1.5 million tons), rainfed agriculture less (≈0.2-0.3 million tons), and residential areas minimal (<0.01 million tons). Moran's I values (0.35-0.54) confirmed strong spatial dependence. Hotspot zones expanded from 28.93% in 2003 to 32.90% in 2050, while coldspots also grew slightly, indicating an increase in spatial polarization. Higher elevations and moderate slopes generally store more Carbon due to denser forest cover and reduced human activity.

Conclusion: The Kojur Watershed exhibits a stable, clustered pattern of Carbon storage. Hotspot zones serve as vital Carbon reservoirs for climate mitigation. Preserving these areas and restoring low-Carbon zones offer a strategic path for sustainable resource management and enhanced ecosystem services.

Keywords: Geographic Information Systems (GIS); Hotspot and Coldspot Analysis; Kojur Watershed; Spatial Autocorrelation Analysis.

CITATION LINKS

[1] Li H.W., Li Y.P., Huang G.H., Gao P.P. Identifyi... [2] Memarian H., Akbari M. Prediction of combined ef... [3] Yang L., Shi L., Li J., ... [4] Armenteras D., Murcia ... [5] Mamtimin A., Amar G., Wang Y., Peng J., Sayit H.... [6] Moradi M., Moradi G. Carbon Sequestration of Med... [7] Tilaki G.A., Rahmani R., Hoseini S.A., Vasenev I... [8] Vannini A., Tarasconi... [9] Esmaili R., Amini F. Spatial Analysis of Air Pol... [10] Liu Y., Mei X., Yue L., ... [11] Li Y., Zhang L., Yan J., Wang P., Hu N., Cheng W... [12] Sadat M., Zoghi M., ... [13] Vahedi A.A., Mattagi A. Amount of Carbon sequest... [14] Liu M., Chen Y., Chen K., Chen Y. Progress and h... [15] Wang Z., Wang B., Zhang Y., Qiuliang Z. Dynamic ... [16] Xu D., Yu C., Lin W., ... [17] Zhang Y., Wang X., Zhang L., Xu H., Jung T., Xia... [18] Xu H., Demetriades A., Reimann C., Jiménez J.J., ... [19] Abolmaali S.M., Tarkesh M., Mousavi S.A., Karimz... [20] Joloro H., Dianati Tilaki G.A., Memarian H., Koo... [21] Azad B., Afzali S.F., ... [22] Kohestani N., Rastgar S., Heydari G., Jouibary S... [23] Kooch Y., Moghimian N., ... [24] Wulder M.A., Masek J.G., Cohen W.B., Loveland T. ... [25] Hajibigloo M., Sheikh V.B., Memarian H., Komaki ... [26] Eslami A., Anvari S., Karimi N., Mohamadi S. App... [27] Digra A., Kaushal A., ... [28] Sakizadeh M., Milewski A. ... [29] Memarian H., Shahrokhi Y., ... [30] Memarian H., Balasundram ... [31] Leta M.K., Demissie ... [32] Atef I., Ahmed W., Abdel-Maguid R.H. Future land... [33] Wu Z., Liu X., Cheng S., Yang C., Wang Z., Liu Y... [34] Du C., Zhou G., Wu N., Gao Y. Grazing exclusion ... [35] VandenBygaart A.J., Bremer E., McConkey B.G., El... [36] Farhadifar A., Dianati Tilaki... [37] Bao K. Carbon Pools, Dynamics and Budget of the ... [38] Xu J., Renaud F.G., Barrett B. ... [39] Zhai Y., Zhai G., ... [40] Kohestani N., Rastgar S., ... [41] Chen Y. New approaches for calculating Moran's i... [42] Hu X., Ma C., Huang... [43] Ding L., Chen K.L., Liu T., Cheng S.G., Wang X. ... [44] Kumar S., Parida B.R. ... [45] Tola A.M., ... [46] Getis A., Ord J.K. The... [47] Shanani H.S., Zarei H. ... [48] Timilsina N., Escobedo F.J., Cropper W.P, Abd-El... [49] Li G., Wu Z., He Y., Chen C., ... [50] Wang X., Zhang W., Zhao X., ... [51] Faraji F., Alijanpour A., ... [52] Fan L, Cai T, Wen Q, Han ... [53] Akrofi M.M. Green hotspots? Unveiling global hot... [54] Hou W., Liu F., Zhang Y., ... [55] Hwang Y.S., Schlueter S., Pradhan B., Um J.S. Un...

Introduction

Changes in Land-use and land-cover (LULC) are major drivers of environmental change at local, regional, and global scales [1,2,3]. Such changes affect both landscape structure and the capacity of ecosystems to store Carbon, particularly through forest and rangeland degradation, which contributes to increased atmospheric CO_2 and climate change [4,5].

Carbon sequestration is a key natural process for reducing greenhouse gases and regulating the global climate [6]. Ecosystems such as forests, rangelands, and agricultural lands can act as Carbon sinks or sources depending on Land-use and management [7,8]. Changes in these ecosystems can significantly impact Carbon dynamics. The distribution and stability of Carbon not only help mitigate climate change but also support ecosystem services such as soil fertility, water quality, and biodiversity [9]. Therefore, it is crucial to understand both the amount and spatial patterns of Carbon over time.

Spatial analysis provides insights into areas of high Carbon sequestration (hot spots) and low Carbon sinks (cold spots) [10], which are essential for guiding conservation priorities and land-use planning [11,12]. The spatial configuration and fragmentation of land-cover also affect Carbon stability, with extensive, continuous forests and grasslands storing more Carbon than fragmented landscapes [13,14,15]. Ecosystem services models, particularly InVEST, integrate LULC data with Carbon coefficients to produce spatial maps of Carbon stocks and track changes over time, thereby supporting the identification of critical Carbon storage areas and the assessment of the ecological consequences of land-use change [16,17].

To further enhance spatial interpretation, InVEST outputs are often combined with geostatistical tools such as Moran's I and Getis-Ord Gi. Moran's I is a widely recognized measure of spatial autocorrelation, used to determine whether Carbon sequestration patterns are clustered, dispersed, or randomly distributed. In contrast, the Getis-Ord Gi statistic identifies statistically significant hotspots and coldspots, highlighting areas with notably high or low Carbon concentrations [14].

A growing body of research at both global and national levels has explored the impact of land-use change on Carbon storage. For example, Xu et al. [18] utilized data from the GEMAS project alongside hotspot analysis to examine spatial patterns of total organic Carbon (TOC) and its relationship with soil pH across European agricultural landscapes. Their findings revealed a strong link between TOC and both soil fertility and Carbon sequestration potential. High TOC levels were concentrated in northeastern Europe, where soils exhibited lower pH. In comparison, southern regions with higher pH showed reduced TOC patterns that aligned with underlying geochemical and textural soil properties.

In a national context, Abolmaali et al. [19] applied the InVEST model and Getis-Ord Gi* analysis to evaluate ecosystem services and identify priority conservation areas within the Zayandeh Rud Watershed. Their study found that Land-use changes, particularly the expansion of low-yield agricultural lands and urban development, had led to declines in ecosystem services, including reduced Carbon storage, increased soil erosion, and reduced habitat quality. Hotspot analysis revealed that 21.5%, 39.3%, and 16.9% of the watershed area were statistically significant zones for Carbon storage, soil conservation,

and habitat integrity, respectively.

Similarly, Joloro et al. [20] conducted a spatiotemporal evaluation of land-use dynamics and restoration interventions in the Kojur Watershed. Their results indicated that forest cover experienced the most notable increase, rising by 5.75% in 2035 and 10.99% in 2050 compared to 2023. Afforestation and vegetation rehabilitation efforts substantially boosted Carbon sequestration across multiple ecosystem compartments, including aboveground biomass, litter, belowground biomass, and soil Carbon pools.

While most Carbon sequestration studies in Iran have concentrated on quantifying sequestration rates over different time periods [21,22], they have largely neglected the spatial heterogeneity and distributional patterns of Carbon storage. This study aims to fill that gap by examining the spatial dynamics of Carbon sequestration within the Kojur Watershed and identifying zones with the highest and lowest sequestration potential over time. The main objective of this study is to analyze the spatial heterogeneity of Carbon sequestration in the Kojur Watershed and to identify priority hotspots and coldspots under past and future Land-use scenarios. Given the critical role of land-use monitoring in understanding Carbon dynamics, particularly in the context of environmental sustainability and natural resource management, the outcomes of this study offer valuable insights. They not only clarify the interplay between land-use change and spatial Carbon distribution but also provide actionable data to support the prioritization of ecologically sensitive areas and inform long-term strategies for sustainable resource management.

Unlike previous studies that mainly quantified total Carbon stocks at single time points [19,20], this study integrates historical and projected land-use scenarios (2003-2050), spatial autocorrelation, and hotspot/coldspot analysis using InVEST. This allows identification of priority areas for Carbon conservation and restoration, providing actionable insights for sustainable watershed management.

Materials & Methods

Study Area

The Kojur Watershed spans approximately 432.85 km^2 and is located within the Nur and Nowshahr counties of Mazandaran Province, northern Iran (Figure 1). The region experiences a Mediterranean and cold semi-humid climate, as classified by the Emberger method [23], with an average annual precipitation of 456.2 mm and a mean actual evapotranspiration of 360 mm. The average temperature across the watershed is 9.7°C. Topographically, the area features a mean elevation of 1789 meters and an average slope of 22.3%. Land-use and land-cover within the watershed are varied, comprising forested areas, irrigated farmland, rainfed croplands, rangelands, and residential zones. In recent decades, the landscape has undergone notable transformations, primarily due to the conversion of forested lands into residential developments and rainfed agricultural fields. These changes have had significant ecological implications, particularly for Carbon storage and ecosystem function [20].

Research Method

Data and Information Sources

• Land-use and land-cover (LULC) Mapping LULC maps for the years 2003, 2013, and 2023 were generated using Landsat satellite imagery obtained from the USGS database.

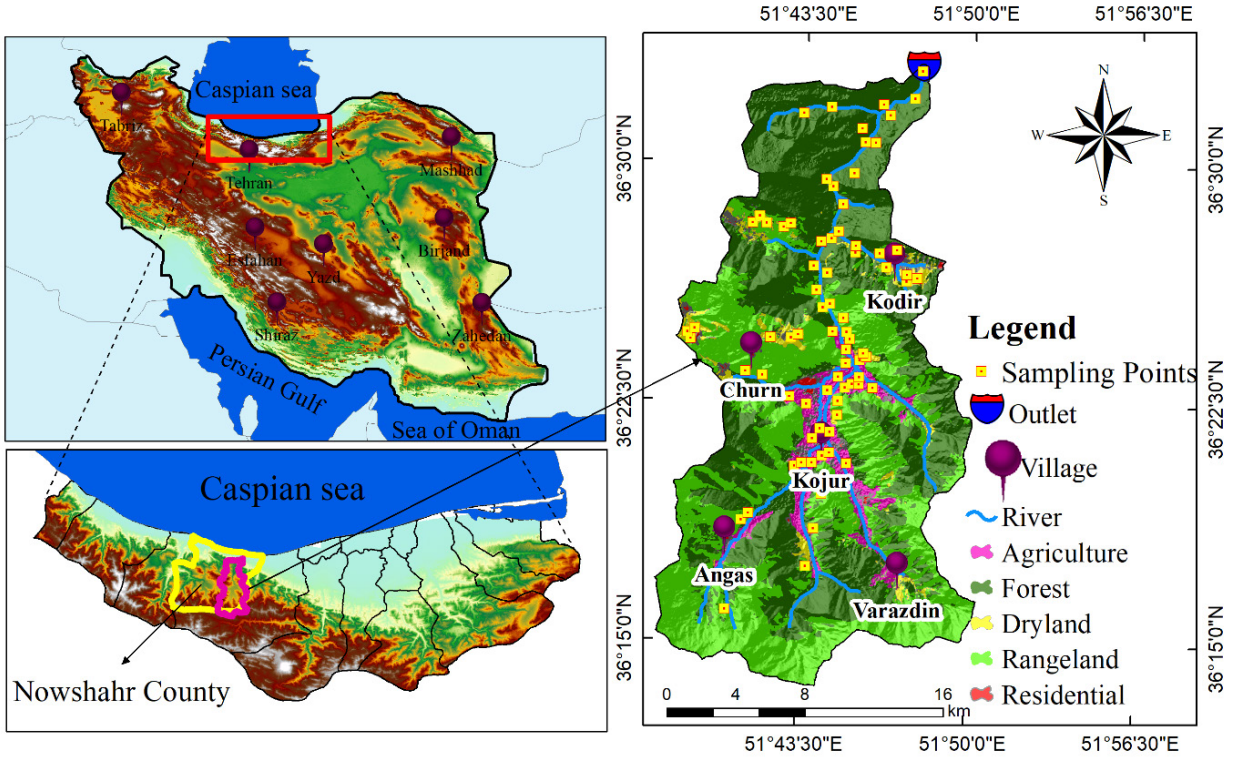

Figure 1) Geographical location of the Kojur Watershed within Iran's political boundaries.

Landsat imagery provides multispectral data at moderate spatial resolution (30 m) and a long-term, continuous archive, which is widely used for detecting land-use and land-cover changes over large areas and across multiple decades [24]. Its availability, consistency, and spectral quality make it suitable for spatiotemporal analysis of Carbon stock dynamics. To classify land-cover changes, two methodological frameworks, including pixel-based classifiers (i.e., Minimum Distance Classifier (MDC), Maximum Likelihood Classifier (MLC), Artificial Neural Network (ANN), and Support Vector Machine (SVM)) and object-based classifiers (i.e., Nearest Neighbor (KNN) and SVM) were applied. Following an accuracy assessment using 350 ground control points, the most reliable classification approach was selected. Subsequent analysis of LULC transitions was conducted using the Land Change Modeler (LCM) within TerrSet software, enabling calculation of change rates and class-specific transitions [25,26,27,28]. To project future land-use dynamics in the Kojur Watershed, the Ca-Markov model, a hybrid approach combining Markov chain analysis with cellular automata, was employed [29]. LULC maps from 2013 and 2023 served as input layers for the LCM module in IDRISI, which was used to simulate land-cover scenarios for 2035 and 2050 [30,31,32].

• Carbon Stock Assessment Carbon stocks were estimated across four primary ecosystem compartments: aboveground biomass (aerial plant structures), belowground biomass (roots), litter, and soil organic Carbon. Soil sampling was conducted using a stratified random approach [33]. The current LULC maps were segmented into 10 km^2 grid cells [34], and random sampling was performed within each cell. For forest, rangeland, and agricultural land-uses, 20 randomly selected

grids were sampled, with three soil cores collected from each grid to a depth of 30 cm (240 soil cores). Residential areas were excluded from Carbon stock calculations, as they were assumed to have negligible storage capacity [35]. Litter and aboveground biomass samples were collected, dried, and weighed to determine Carbon content. Root biomass was extracted from the soil profile by excavation, then washed and weighed. These procedures enabled direct quantification of Carbon across the aboveground, belowground, and litter pools [36,37].

• Image Processing and Spatial Analysis Satellite imagery was processed, and maps were generated using ENVI and ArcGIS Software. Carbon sequestration modeling was performed using version 3.12 of the InVEST tool, while spatial analyses, including pattern detection and hotspot identification, were conducted in ArcGIS.

Carbon Sequestration Estimation using InVEST

To assess Carbon sequestration within the Kojur Watershed, this study utilized the Carbon Storage and Sequestration module of the InVEST model, a widely recognized tool for evaluating ecosystem services [38]. InVEST offers a robust and scientifically validated framework for spatial modeling of Carbon stocks by integrating Land-use and land-cover (LULC) data with Carbon inventories across four key Carbon pools: aboveground biomass, belowground biomass, litter, and soil organic Carbon [39,40]. Carbon in each pool was estimated through field sampling, sample drying and weighing, and organic Carbon determination. To estimate Carbon storage in soil, litter, and above- and belowground biomass, field sampling was conducted. Soil samples were collected to a depth of 30 cm from 20 random plots per land-use type (forest, pasture, irrigated, and rainfed cropland), with three samples per plot. Additionally, 20 samples per pool (aboveground biomass, litter, belowground biomass) were collected for each land-use type and transported to the laboratory. Samples were dried and sieved, and their organic Carbon content was determined by combustion and standard conversion equations. For biomass and litter, plant samples were collected, dried, weighed, and their organic Carbon was calculated using a conversion factor from organic matter to Carbon. The Carbon values used in this study were derived from a previous investigation by the same authors [20] and served as input for subsequent spatial analyses.

Spatial and Statistical Analyses

To explore spatial patterns and temporal shifts in Carbon sequestration, a series of analytical procedures was conducted:

1. Spatial Autocorrelation Analysis (Moran's I): Spatial autocorrelation analysis is a fundamental technique used to evaluate the degree of similarity among neighboring spatial units based on a given variable [41]. It is typically divided into global and local measures. Global Moran's I provides insight into whether spatial data exhibit clustered, dispersed, or random distribution patterns. In this study, the Global Moran's I statistic was applied to detect spatial structure in Carbon sequestration data. Moran's I values, along with associated Z-scores and p-values, were calculated across a range of distance bands. To determine the optimal search radius (Distance Band), the first statistically significant Z-score peak ($p<0.05$) was selected, identified as 1042 meters for the Kojur Watershed. This distance was chosen to maximize spatial coherence and improve the accuracy of cluster pattern detection.

The Moran's I index was calculated using Eq. (1), following the methodology outlined by Hu et al. [42].

$$I = \frac{n}{W} \times \frac{\sum_{i=1}^{n}\sum_{j=1}^{n} W_{ji}\left(x_i - \bar{x}\right)\left(x_j - \bar{x}\right)}{\sum_{i=1}^{n}\left(x_i - \bar{x}\right)^2} \quad \text{Eq. (1)}$$

where n is the total number of spatial units analyzed, x_i and x_j are observed values at spatial location i and j, is the mean of all observed values across the study area, W_{ij} is a spatial weight representing the degree of spatial interaction between locations j, and W is the sum of all spatial weights in the matrix. In this study, Carbon stocks were categorized into five classes based on local spatial autocorrelation, which assesses the degree of similarity among neighboring spatial units. The Local Moran's I index, ranging from -3 to +3, was used to quantify these relationships. Positive values (greater than zero) indicate statistically significant positive spatial autocorrelation, suggesting that adjacent areas share similar Carbon storage characteristics and form spatial clusters. Negative values (less than zero) reflect inverse relationships, in which neighboring units exhibit contrasting Carbon storage patterns, forming clusters with opposing traits. A value near zero implies minimal or no spatial autocorrelation, indicating a random distribution of Carbon stocks across the landscape.

2. Hotspot Analysis (Getis-Ord Gi)*: The Getis-Ord Gi* statistic is a widely applied local spatial autocorrelation measure used to detect clustering patterns of specific attributes in geospatial datasets. Often referred to as Hotspot Analysis [43], this method compares the value of each spatial unit to the average values of its surrounding neighbors to identify statistically significant concentrations. Areas with notably high values are classified as hotspots, while those with low values are designated as coldspots [44].

One of the key strengths of the Getis-Ord Gi* statistic lies in its ability to capture localized spatial variation, distinguishing between clusters of high and low values within a defined region. This contrasts with global measures such as Moran's I, which provide an overall assessment of spatial autocorrelation but may overlook finer-scale patterns [45]. The results of the Gi* analysis include both the Gi* value and its corresponding z-score, which together indicate the magnitude and direction of spatial clustering. High positive Gi* values and z-scores signal strong clustering of high values, whereas low negative scores indicate clustering of low values.

Statistical significance was determined based on the Z-score and associated p-value for each spatial unit. Specifically:

- A Z-score≥2 with p<0.05 was considered a significant hotspot (high concentration of Carbon).
- A Z-score≤-2 with p<0.05 was considered a significant coldspot (low concentration of Carbon).
- Values with Z-scores between -2 and 2 were considered not statistically significant, indicating no meaningful spatial clustering [46].

The Gi* statistic is computed using Eq. (2), offering a robust framework for detailed spatial pattern analysis [46].

$$Gi^* = \frac{\sum_{i=1}^{n} w_{ji}x_j - \bar{X}\sum_{j=1}^{n} w_{ji}}{s\sqrt{\frac{\left[n\sum_{j=1}^{n} w_{ji}^2 - \left(\sum_{j=1}^{n} w_{ij}\right)^2\right]}{n-1}}} \quad \text{Eq. (2)}$$

where n is the total number of spatial units analyzed, x_j is the value of the attribute at location j, w_{ij} is the spatial weight between locations i and j, is the mean of the attribute

across all locations, S is the standard deviation of the attribute values, and n is the total number of spatial units.

3. Hotspot mapping: The results of the Getis-Ord Gi* analysis were visualized through maps showing spatial clusters of high (hotspots) and low (coldspots) Carbon values. Areas with significant positive Z-scores were identified as hotspots, while areas with negative Z-scores were designated as coldspots. A color gradient from red to orange for hotspots and from blue to green for coldspots was applied to improve interpretability and support spatially informed decision-making in land management.

Moran's I and Getis-Ord Gi* statistics are appropriate tools for detecting spatial clustering and identifying hotspots and coldspots, aligning with the study's objective of assessing spatial heterogeneity of Carbon sequestration in the Kojur Watershed.

Findings

Land-Use and Land-Cover Dynamics

Figure 2 presents both historical and projected Land-use and land-cover (LULC) changes within the Kojur Watershed. Analysis of LULC transitions from 2003 to 2023 revealed a notable expansion of forested areas, with an increase of approximately 1901 hectares (Table 1). Rainfed agricultural lands and residential zones also showed considerable growth. Conversely, rangelands experienced the most pronounced decline, with a net reduction of 3047 hectares. Projections based on the Markov chain model suggest continued shifts in land-use patterns through 2035 and 2050. Forest cover is expected to grow by 5.75% and 10.99%, equivalent to 1285 and 2590 hectares, respectively. Rainfed agriculture and residential development are also anticipated to expand.

Meanwhile, certain land-cover classes are projected to undergo significant net losses 11.65% and 27.90%, corresponding to reductions of 1770 and 3701 hectares, respectively. These spatial trends underscore substantial transformations in forest expansion, agricultural intensification, and urbanization, which collectively inform the modeling of Carbon sequestration potential. A more detailed account of this analysis and its broader implications is available in the study by Joloro et al. [20].

To assess the accuracy of the CA-Markov model, the simulated land-use map for

Table 1) Characteristics of Land-use changes in the Kojur Watershed from 2003 to 2023.

Types of Land-Use		Agriculture	Rainfed Farming	Forest	Rangeland	Residential Zone
2003	Area (ha)	3009.86	821.10	19067.98	20017.72	368.23
	Proportion (%)	6.95	1.90	44.05	46.25	0.85
2013	Area (ha)	3893.57	787.63	19573.08	18593.77	436.85
	Proportion (%)	9.00	1.82	45.22	42.96	1.01
2023	Area (ha)	3019.45	1851.22	20968.98	16970.26	474.98
	Proportion (%)	6.98	4.28	48.44	39.21	1.10
Area Change (ha)		9.58	1030.12	1901.00	-3047.46	106.75
Rate of Area Change (%)		0.32	125.46	9.97	-15.22	28.99

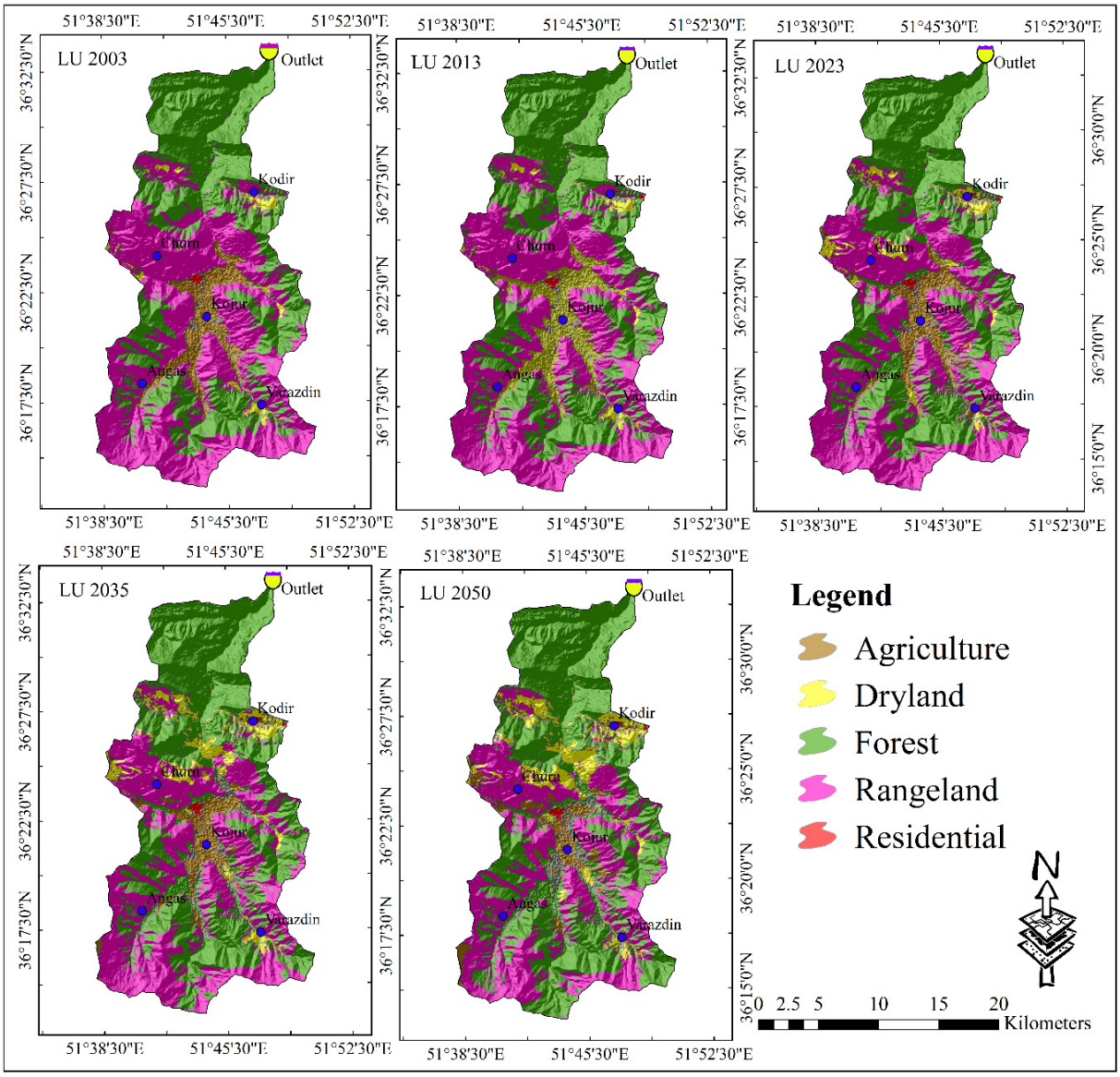

Figure 2) Land-use and land-cover change maps for 2003, 2013, 2023, and projections for 2035 and 2050.

the latest year was compared with the corresponding observed map, and standard validation metrics such as overall accuracy and kappa coefficient were calculated. The overall accuracy and kappa coefficient for the 2023 land-use map were 95.77% and 0.96, respectively. An accuracy above 85% is generally considered sufficient for satellite image classification [47]; thus, the 2023 land-use map is deemed appropriately classified

Carbon Sequestration Assessment using InVEST

Carbon sequestration across the Kojur Watershed was evaluated using the Carbon Storage and Sequestration module of the InVEST software suite. For each time period under study, the model generated spatial distribution maps of Carbon stocks (Figure 3). The analysis revealed that forested areas consistently contributed the largest share of Carbon storage between 2003 and 2023, with a clear upward trajectory. In contrast, rangelands exhibited a decline in Carbon sequestration capacity over the same period. Estimated total Carbon stocks for the watershed were 4026300.66 tons

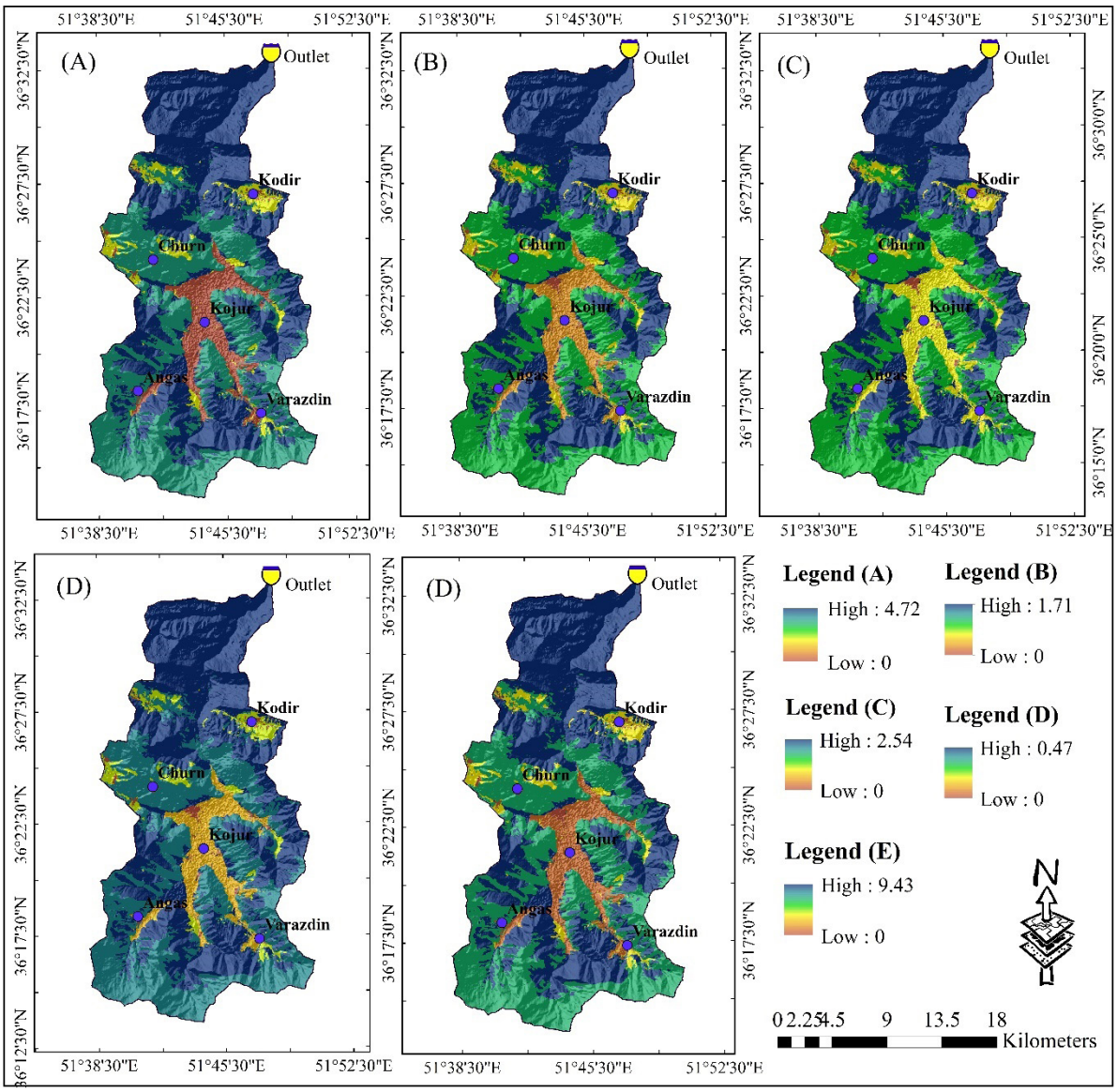

Figure 3) Carbon sequestration maps for 2003, 2013, 2023, and projections for 2035 and 2050.

in 2003, 3999632.57 tons in 2013, and 4029007.23 tons in 2023. Forecasts for 2035 and 2050 indicate continued growth, with projected totals reaching 4042708.63 tons and 4051239.71 tons, respectively. These findings highlight the pivotal role of forest conservation and vegetation management in enhancing Carbon sequestration and mitigating the impacts of climate change. The Carbon distribution maps produced by the InVEST model served as foundational inputs for subsequent spatial analyses, including Global Moran's I and Hotspot Analysis. A detailed account of the analytical framework and results is provided in Joloro et al. [20].

Spatial Autocorrelation (Moran's I)

Spatial autocorrelation analysis using Moran's I revealed that Carbon sequestration patterns in the Kojur Watershed remained significantly clustered across all five time points: 2003, 2013, 2023, 2035, and 2050. Moran's I values ranged from 0.35 (Z=154.61) in 2003, indicating moderate clustering, to 0.54 (Z=237.54) in 2013, reflecting stronger clustering of high-Carbon areas. In 2023, Moran's I decreased slightly to 0.49

(Z=217.01), followed by projections of 0.48 (Z=215.15) in 2035 and 0.47 (Z=204.49) in 2050, indicating a modest weakening of spatial cohesion. Throughout the period, all p-values were below 0.05, confirming statistically significant clustering. The overall trend suggests that Carbon-rich zones remained concentrated, with slight dispersion over time likely influenced by Land-use changes, vegetation fragmentation, human activities, and climate variability (Table 2).

Overall, the results indicate that the Kojur Watershed exhibits a stable spatial clustering pattern in Carbon stocks, with high concentration zones (hotspots) consistently identifiable and traceable over time. These findings highlight the importance of recognizing and protecting these critical areas to support sustainable natural resource management and enhance ecosystem services. Such insights can serve as a foundation for future policy development and strategic planning efforts.

Hotspot Analysis

This study examined spatial variations in Carbon stock distribution across the Kojur Watershed from 2003 to 2050, using the Getis-Ord Gi* statistic in ArcGIS. The analysis revealed statistically significant patterns of Carbon sequestration, identifying clusters of both high and low Carbon accumulation. Figure 4 displays the hotspot and cold spot maps for Carbon sequestration, highlighting spatial clustering across five time points: 2003, 2013, 2023, 2035, and 2050. To interpret the hotspot analysis results, Gi* values were categorized into five distinct classes, as outlined in Table 3. The classification scheme is as follows:

Gi ≥ 2*: Indicates statistically significant hotspot areas with elevated Carbon sequestration.

Gi ≤ -2*: Denotes cold spots zones with markedly low Carbon accumulation.

Gi values between -2 and +2*: Considered statistically insignificant and interpreted as non-clustered areas.

To enhance visual clarity, the maps were color-coded: red for hotspots, blue for cold spots, and gray for areas lacking spatial clustering.

Table 4 summarizes the outcomes of the Getis-Ord Gi* hotspot analysis, highlighting temporal changes in the spatial distribution of Carbon sequestration zones within the Kojur Watershed from 2003 to 2050. Over this period, the proportion of the watershed identified as Carbon sequestration hotspots increased modestly from 28.93% in 2003 to 32.90% in 2050. This upward trend suggests a growing concentration of Carbon stocks in

Table 2) Spatial autocorrelation of Carbon sequestration in the Kojur Watershed across different years.

Year	Moran's I	Z-score	P-value	Pattern Interpretation
2003	0.35	154.61	0.000	Clustered
2013	0.54	237.54	0.000	Clustered
2023	0.49	217.01	0.000	Clustered
2035	0.48	215.15	0.000	Clustered
2050	0.47	204.49	0.000	Clustered

Table 3) Classification of Carbon sequestration hotspots and cold spots based on Gi* statistic.

Category	Gi* Range	Interpretation	Suggested Color
Strong Hotspot	Gi* ≥ 3	Very High Carbon Sequestration	Dark Red
Moderate Hotspot	2 ≤ Gi* < 3	High Carbon Sequestration	Light Red /Orange
Not Significant	-2 < Gi* < 2	Random Distribution	Gray
Moderate Coldspot	-3 < Gi* ≤ -2	Low Carbon Sequestration	Light Blue /Cyan
Strong Coldspot	Gi* ≤ -3	Very Low Carbon Sequestration	Dark Blue

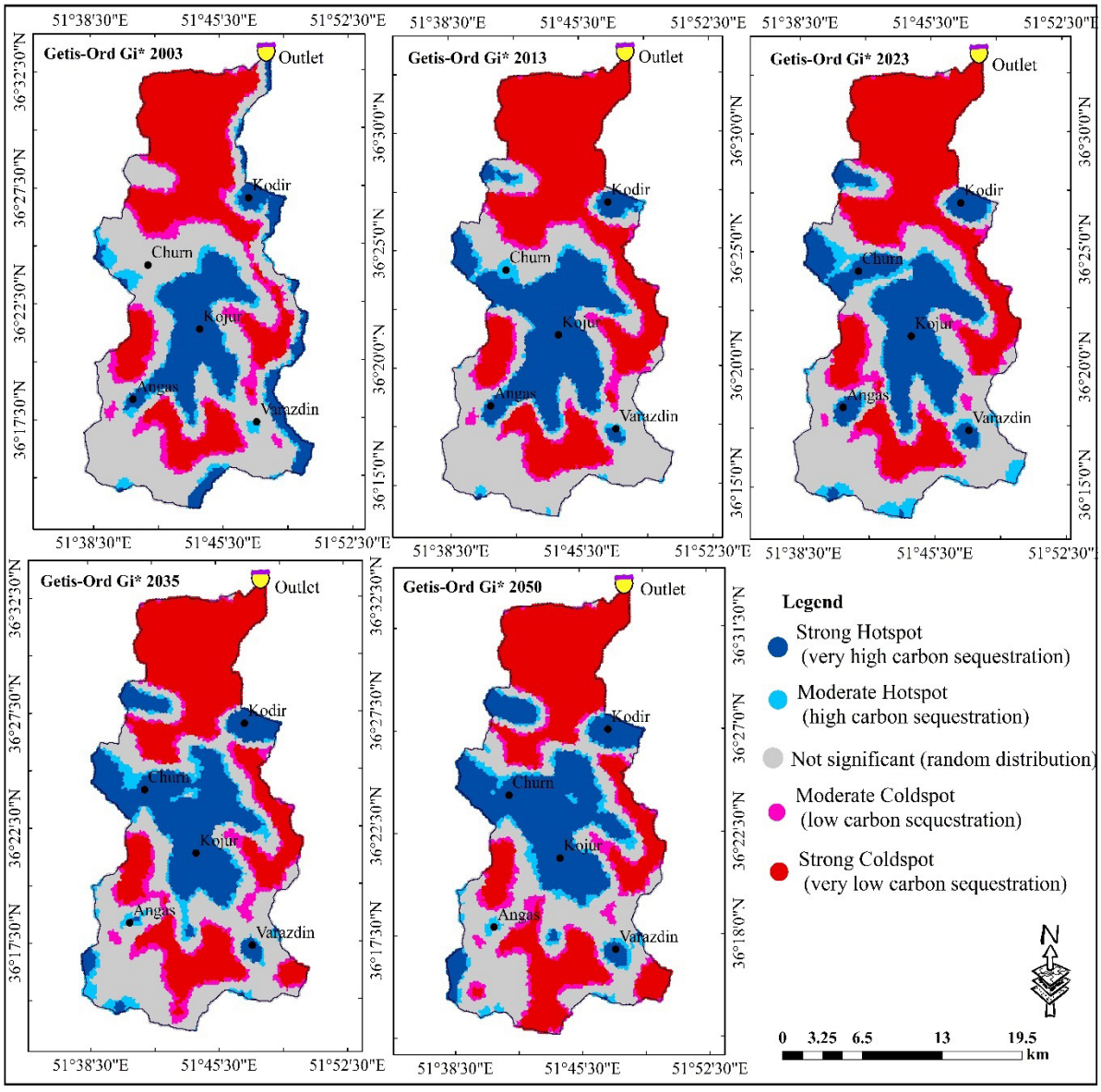

Figure 4) Spatial distribution of Carbon stocks in the Kojur Watershed (2003, 2013, 2023, and projections for 2035 and 2050).

Table 4) Temporal changes in the percentage of the Kojur Watershed area classified as hotspot, cold spot, and non-significant zones.

Year	Hotspot Area (%)	Coldspot Area (%)	Non-significant Area (%)
2003	28.93	17.97	53.10
2013	32.56	18.51	48.93
2023	31.81	19.79	48.40
2035	32.29	20.45	47.25
2050	32.90	21.54	45.56

ecologically significant areas and reflects the persistence of spatial clustering patterns. Similarly, coldspot areas, with notably low Carbon accumulation, also expanded, rising from 17.97% in 2003 to 21.54% in 2050. This increase may be linked to shifts in Land-use and human activities, or to declining vegetation cover in certain parts of the watershed.

In contrast, the share of statistically non-significant (ordinary) areas decreased from 53.10% to 45.56% over the same period. This decline indicates a gradual expansion of both hotspot and cold spot zones, reinforcing the notion that Carbon stock distribution has become more spatially structured and stable over time. Taken together, these findings underscore the emergence of distinct spatial patterns in Carbon sequestration, with high- and low-accumulation zones becoming increasingly concentrated. Such insights are valuable for guiding sustainable natural resource management and prioritizing conservation efforts in ecologically sensitive regions.

Discussion

The spatial autocorrelation analysis, based on Moran's I statistic, reveals that Carbon sequestration within the Kojur Watershed has consistently exhibited significant spatial clustering across all assessed years 2003, 2013, 2023, 2035, and 2050. With Moran's I values ranging from 0.35 to 0.54 and p-values below 0.05, the results confirm that Carbon stocks are not randomly distributed but are instead concentrated in well-defined spatial clusters [48].

A notable increase in Moran's I from 0.35 in 2003 to 0.54 in 2013 suggests a strengthening of spatial cohesion among high Carbon zones, likely driven by improvements in forest cover or rising biomass density in specific regions. However, a slight decline in Moran's I values from 0.49 to 0.47 in the following years indicates a modest weakening of this spatial cohesion. This shift may be attributed to land-use changes, fragmentation of forest and rangeland ecosystems, anthropogenic disturbances, or climate-related stressors [49]. These patterns are consistent with findings from other watershed studies. For example, Abolmaali et al. [19] and Wang et al. [50] similarly observed that Carbon sequestration tends to form spatial clusters, with their configuration influenced by Land-use transitions and management interventions.

An upward shift in Moran's I from 0.35 in 2003 to 0.54 in 2013 reflects a notable increase in the spatial concentration and cohesion of areas with elevated Carbon stocks. During this period, zones with denser biomass and more robust forest cover emerged as

central nodes within the clustering pattern. However, the slight decline in Moran's I values observed in subsequent years (from 0.49 to 0.47) points to a gradual weakening of spatial cohesion. This change is likely the result of multiple interacting factors, including land-use transformation, fragmentation of vegetative cover, expansion of agricultural and residential developments, and the cumulative effects of human activity and climate variability [49,51]. In addition, topographic factors play an essential role in shaping the spatial distribution of Carbon sequestration. Areas located at higher elevations and with moderate slopes generally show higher Carbon storage due to higher forest density and limited human disturbance.

In contrast, lowland areas and gentle slopes are more prone to agricultural conversion and settlement expansion, resulting in lower Carbon accumulation [20]. These findings confirm the strong association between topography and spatial Carbon clustering. These trends align with findings from comparable studies. For instance, Zhang et al. [17] reported that shifts in land-use and management strategies can substantially alter the spatial distribution of Carbon stocks, either reinforcing or disrupting the integrity of clustering patterns.

The hotspot analysis using the Getis-Ord Gi* statistic confirms spatial clustering of Carbon sequestration across the Kojur Watershed. The results indicate that zones with elevated Carbon stocks identified as hotspots are not randomly distributed but are spatially concentrated, serving as critical areas for Carbon capture and long-term storage. In contrast, coldspot areas with lower Carbon stock values are more scattered and appear to be strongly influenced by land-use changes and human activities. Regions that do not exhibit statistically significant clustering suggest a more random spatial distribution of Carbon stocks, reflecting variability in ecological conditions or management intensity. Overall, the findings highlight the spatial heterogeneity of Carbon distribution and underscore distinct clustering patterns. These insights underscore the importance of prioritizing hotspot zones in conservation planning and resource management. This spatial pattern is consistent with the findings of Zhang et al. [52], who reported that a combination of land-use dynamics, environmental factors, and management interventions shapes Carbon sequestration hotspots.

An examination of changes in the spatial extent of hotspot and coldspot areas reveals a clear and consistent trend. Between 2003 and 2050, the proportion of Carbon sequestration hotspots increased from 28.93% to 32.90%, reflecting a growing concentration and long-term stability of Carbon stocks in ecologically significant zones. At the same time, coldspot areas, regions with lower Carbon accumulation, expanded from 17.97% to 21.54%, likely driven by vegetation degradation or shifts in land-use across parts of the watershed [18]. This increase in coldspot areas is mainly associated with the conversion of forests and rangelands into agricultural and built-up areas. Such land-use transitions reduce vegetation cover and soil organic matter, thereby diminishing the potential for Carbon sequestration. Ecologically, this trend reflects a decline in ecosystem functioning and resilience, particularly in areas exposed to deforestation and overgrazing. From a socio-economic standpoint, the expansion of agricultural and urban regions indicates

growing human pressure on natural ecosystems, which, while supporting short-term economic development, can undermine long-term environmental sustainability [53]. Meanwhile, the share of statistically non-significant areas declined from 53.10% to 45.56%, suggesting that spatial clustering has become more pronounced over time. This trend enhances the detectability and monitoring of both hotspot and coldspot zones. These findings are consistent with previous studies conducted in comparable landscapes, which have shown that Carbon stock distribution tends to follow clustered spatial patterns [54,55] and that the concentration of Carbon-rich areas is highly responsive to land-use dynamics and anthropogenic pressures [2,20]. Notably, identifying these zones provides a valuable foundation for conservation prioritization and resource management planning. It enables the formulation of targeted strategies to safeguard ecosystem services and mitigate the adverse effects of climate change. Taken together, the insights from Moran's I and hotspot/coldspot analyses suggest that the Kojur Watershed exhibits a stable, spatially clustered pattern of Carbon distribution. These key zones represent critical areas for focused conservation efforts and sustainable natural resource governance.

Although the study provides a detailed assessment of Carbon sequestration patterns in the Kojur Watershed, it should be noted that it has some limitations. First, uncertainties in satellite-based land-use classification and Carbon stock estimation may affect the accuracy of results. Second, socio-economic factors and biodiversity indicators were not incorporated, which could provide additional insights into land-use dynamics and ecosystem services. Future research could integrate these variables and explore scenario-based management strategies to enhance the robustness and applicability of findings.

Conclusion

The findings of this study demonstrate that the spatial pattern of Carbon sequestration in the Kojur Watershed has remained significantly clustered over the past two decades and is projected to persist through 2050. Moran's I values across all examined years ranged from 0.35 to 0.54, accompanied by statistically significant Z-scores and p-values ($p<0.05$), indicating sustained spatial cohesion in Carbon stock distribution throughout the watershed. The increase in Moran's I from 0.35 in 2003 to 0.54 in 2013 reflects a growing concentration and cohesion among high-Carbon zones. The subsequent slight decline in values (from 0.49 to 0.47) suggests minor shifts in spatial clustering, likely driven by land-use changes, vegetation fragmentation, and anthropogenic pressures.

Hotspot analysis further revealed that the area of high Carbon sequestration zones (hotspots) expanded from 28.93% in 2003 to 32.90% in 2050, while low-Carbon zones (coldspots) also increased in extent. These trends indicate not only the persistence of Carbon distribution patterns but also a gradual intensification of spatial clustering, with certain regions playing a pivotal role in Carbon capture and retention. From a management perspective, identifying and protecting key Carbon sequestration hotspots alongside targeted restoration and enhancement of coldspot areas can serve as a strategic foundation for conservation policies, sustainable resource management,

and the improvement of ecosystem services. The results underscore the importance of intelligent land-use planning and vegetation enhancement in maintaining and boosting Carbon sequestration capacity, while mitigating the impacts of climate change in similar watershed systems.

The simultaneous expansion of both high- and low-Carbon zones underscores the urgent need for integrated planning approaches that prioritize protecting Carbon-rich areas and rehabilitating Carbon-deficient regions. To translate these findings into practical actions, several policy and management measures are recommended for the Kojur Watershed. Community-based forest management programs should be promoted to engage local stakeholders in protecting high-Carbon zones. Land-use zoning regulations need to be strengthened to prevent agricultural expansion and uncontrolled development in areas with high Carbon storage potential. In addition, reforestation, soil restoration, and sustainable rangeland management initiatives should be prioritized in degraded or low-Carbon regions. Implementing these measures can enhance Carbon sequestration capacity, improve ecosystem resilience, and contribute to long-term sustainable land-use planning in the watershed.

Acknowledgments

The authors express their gratitude to all those who contributed to the success of this research.

Authors' Contribution

H Joloro: Sampling and laboratory analysis, Writing – original draft, Software. **Gh.A Dianati Tilaki:** Sampling, Revising and editing, Supervision. **H Memarian:** Software, Methodology. **Y Kooch:** Writing-revision and editing.

Ethical Permission

The authors demonstrate that they have adhered to the accepted ethical principles of the study.

Funding/ Support

This research received no specific grant from any funding agency in the public, commercial, or not-for-profit sectors.

Conflict of interest

The authors declare that they have no conflicts of interest.

AI Use Declaration

Artificial intelligence (ChatGPT, 2025) tools were used during the initial drafting and organization of this manuscript. However, all scientific content, arguments, data analyses, and interpretation of results were conducted by the authors, and the scientific accuracy of the material was reviewed and approved by them. Artificial intelligence played no role in data generation or scientific decision-making.

References

1. Li H.W., Li Y.P., Huang G.H., Gao P.P. Identifying optimal Land-use patterns using a copula-based interval stochastic programming model for urban agglomeration under uncertainty. Ecol. Eng. 2020; 142(1): 105616.
2. Memarian H., Akbari M. Prediction of combined effect of climate and Land-use changes on soil erosion in Iran using GloSEM data. J. Ecohydrol. 2021; 8(2): 513-534.
3. Yang L., Shi L., Li J., Kong H. Spatio-temporal pattern change of LULC and its response to climate in the Loess Plateau, China. Sci. Rep. 2024; 14(1): 23202.
4. Armenteras D., Murcia U., González T.M., Barón O.J., Arias J.E. Scenarios of Land-use and land-cover change for NW Amazonia: Impact on forest intactness. Glob. Ecol. Conserv. 2019; 17(1): e00567.
5. Mamtimin A., Amar G., Wang Y., Peng J., Sayit H., Gao J., Zhang K., Song M., Aihaiti A., Wen C., Yang F. Assessment of CO2 fluxes in the hinterland of the Gurbantunggut Desert and its response to climate change. J. Environ. Manage. 2025; 375(1): 124351.
6. Moradi M., Moradi G. Carbon Sequestration of

Mediterranean Tree Species in the Zagros Forest of Iran. ECOPERSIA 2024; 12(4): 351-361.
7. Tilaki G.A., Rahmani R., Hoseini S.A., Vasenev I. The effect of land management on Carbon sequestration in salty rangelands of Golestan Province, Iran. Acta Ecol. Sin. 2022; 42(1): 82-89.
8. Vannini A., Tarasconi D., Pietropoli F., Forte T.A., Grillo F., Carbognani M., Petraglia A. Effects of Wood-Derived Biochar on Soil Respiration of a European Beech Forest Under Current Climate and Simulated Climate Change. Forests 2025; 16(3):474.
9. Esmaili R., Amini F. Spatial Analysis of Air Pollutants Carbon Monoxide in Mashhad. Environ. Res. 2022; 13(25):249-266.
10. Liu Y., Mei X., Yue L., Zhang M. Response of Carbon storage to land-use change and multi-scenario predictions in Zunyi, China. Sci. Rep. 2025; 15(1): 236.
11. Li Y., Zhang L., Yan J., Wang P., Hu N., Cheng W., Fu B. Mapping the hotspots and coldspots of ecosystem services in conservation priority setting. J. Geogr. Sci. 2017; 27(6):681-696.
12. Sadat M., Zoghi M., Amiri M.J. Investigating the Effects of Some Ecological Indicators of Forest Patches on the Supply of Selected Ecosystem Services (Study Area: Eastern Part of Gilan Province). Geogr. Environ. Plan. 2024; 35(1): 89-110.
13. Vahedi A.A., Mattagi A. Amount of Carbon sequestration distribution associated with oak tree's (*Quercus castaneifolia* CA May) bole in relation to physiographical units of Hyrcanian natural forests of Iran. J. For. Poplar Res. 2014; 21(4): 716-728.
14. Liu M., Chen Y., Chen K., Chen Y. Progress and hotspots of research on land-use Carbon emissions: A global perspective. Sustainability. 2023; 15(9): 7245.
15. Wang Z., Wang B., Zhang Y., Qiuliang Z. Dynamic simulation of multi-scenario land-use change and Carbon storage assessment in Hohhot city based on PLUS-InVEST model. J. Agric. Resour. Environ. 2024; 41(2): 292.
16. Xu D., Yu C., Lin W., Yao J., Zhou W. Spatiotemporal Evolution and Prediction of land-use and Carbon Stock in Shanghai. Land 2024; 13(3): 267.
17. Zhang Y., Wang X., Zhang L., Xu H., Jung T., Xiao L. Changes in Wuhan's Carbon Stocks and Their Spatial Distributions in 2050 under Multiple Projection Scenarios. Sustainability 2024; 16(15): 6684.
18. Xu H., Demetriades A., Reimann C., Jiménez J.J., Filser J., Zhang C., GEMAS Project Team. Identification of the co-existence of low total organic Carbon contents and low pH values in agricultural soil in north-central Europe using hot spot analysis based on GEMAS project data. Sci. Total Environ. 2019; 678(1): 94-104.
19. Abolmaali S.M., Tarkesh M., Mousavi S.A., Karimzadeh H., Pourmanafi S., Fakheran S. Identifying priority areas for conservation: using ecosystem services hotspot mapping for land-use/land-cover planning in central Iran. Environ. Manag. 2024; 73(5): 1016-1031.
20. Joloro H., Dianati Tilaki G.A., Memarian H., Kooch Y. Spatial-temporal assessment of land-use changes and forest restoration on Carbon sequestration using the InVEST model in Central Alborz, Iran. Model. Earth Syst. Environ. 2025; 11(4): 277.
21. Azad B., Afzali S.F., Francaviglia R. Simulating soil CO2 emissions under present and climate change conditions in selected vegetation covers of a semiarid region. Int. J. Environ. Sci. Technol. 2020; 17(5): 3087-3098.
22. Kohestani N., Rastgar S., Heydari G., Jouibary S.S., Amirnejad H. Monitoring the spatial distribution of soil Carbon sequestration for four decades based on changes in rangeland vegetation conditions (case study: Noorrud watershed in Mazandaran Province). Rangel. Res. Manag. 2021; 15(2): 344-356.
23. Kooch Y., Moghimian N., Wirth S., Noghre N. Effects of grazing management on leaf litter decomposition and soil microbial activities in northern Iranian rangeland. Geoderma. 2020; 361(1): 114100.
24. Wulder M.A., Masek J.G., Cohen W.B., Loveland T.R., Woodcock C.E. Opening the archive: How free data has enabled the science and monitoring promise of Landsat. Remot. Sens. Environ. 2012; 122(1): 2-10.
25. Hajibigloo M., Sheikh V.B., Memarian H., Komaki C.B. Three-dimensional calibration of land-use changes using the integrated model of Markov chain automatic cell in the Gorgan-Rud River Basin. J. RS GIS Nat. 2020; 11(2): 1-26.
26. Eslami A., Anvari S., Karimi N., Mohamadi S. Application of pixel-based and object-based approaches for LULC mapping in Jiroft region, SE Iran. ECOPERSIA 2022; 10(1): 71-83.
27. Digra A., Kaushal A., Loshali D.C. Evaluation of Multi-Sensor Satellite Data Accuracy for LU/LC Classification: Insights from Cartosat-1 and Liss-Iv Imagery In 2021. ECOPERSIA 2024; 12(2): 111-119.
28. Sakizadeh M., Milewski A. Quantifying LULC changes in Urmia Lake Basin using machine learning techniques, intensity analysis, and a combined method of cellular automata (CA) and artificial neural networks (ANN)(CA-ANN). Model. Earth Syst. Environ. 2024; 10(2): 2011-2030.
29. Memarian H., Shahrokhi Y., Tajbakhsh M. Analyzing and modeling urban sprawl and Land-use changes in a developing city using a

CA-Markovian approach. Glob. J. Environ. Sci. Manage. 2016; 2(4): 397-410.
30. Memarian H., Balasundram S.K., Talib J.B., Sung C.T., Sood A.M., Abbaspour K. Validation of CA-Markov for simulation of land-use and cover change in the Langat Basin, Malaysia. J. Geogr. Inf. Syst. 2012; 4(6): 542-554.
31. Leta M.K., Demissie T.A., Tränckner J. Modeling and prediction of land-use land-cover change dynamics based on land change modeler (Lcm) in Nashe watershed, Upper Blue Nile basin, Ethiopia. Sustainability. 2021; 13(7):3740.
32. Atef I., Ahmed W., Abdel-Maguid R.H. Future land-use land-cover changes in El-Fayoum governorate: a simulation study using satellite data and CA-Markov model. Stoch. Environ. Res. Risk Assess. 2024; 38(2): 651-664.
33. Wu Z., Liu X., Cheng S., Yang C., Wang Z., Liu Y., Dong L., Li F., Hao Y. Evaluating the effectiveness of forest type stratification for aboveground biomass inference. Int. J. Appl. Earth Obs. Geoinf. 2025; 143(1): 104829.
34. Du C., Zhou G., Wu N., Gao Y. Grazing exclusion alters Carbon flux of alpine meadow in the Tibetan Plateau. J. Agric. For. Meteorol. 2022; 314, 108774.
35. VandenBygaart A.J., Bremer E., McConkey B.G., Ellert B.H., Janzen H.H., Angers D.A., Carter M.R., Drury C.F., Lafond G.P., McKenzie R.H. Impact of sampling depth on differences in soil Carbon stocks in long-term agroecosystem experiments. Soil Sci. Soc. Am. J. 2011; 75(1): 226-234.
36. Farhadifar A., Dianati Tilaki G.A., Kooch Y. The effects of forest and rangelands covers on accumulation of soil nutrient elements in Kojur Region. J. Plant Res. (Iran. J. Biol.). 2021; 34(3): 706-716.
37. Bao K. Carbon Pools, Dynamics and Budget of the Bruce Peninsula. Electronic Theses and Dissertations (ETDs), Faculty of Graduate Studies. 2024.
38. Xu J., Renaud F.G., Barrett B. Modelling land system evolution and dynamics of terrestrial Carbon stocks in the Luanhe River Basin, China: a scenario analysis of trade-offs and synergies between sustainable development goals. Sustain. Sci. 2022; 17(4): 1323-1345.
39. Zhai Y., Zhai G., Chen Y., Liu J. Research on regional terrestrial Carbon storage based on the pattern-process-function. Ecol. Inform. 2024; 80(1): 102523.
40. Kohestani N., Rastgar S., Heydari G., Jouibary S.S., Amirnejad H. Spatiotemporal modeling of the value of Carbon sequestration under changing land-use/land-cover using InVEST model: A case study of Nour-rud Watershed, Northern Iran. Environ. Dev. Sustain. 2024; 26(6): 14477-14505.
41. Chen Y. New approaches for calculating Moran's index of spatial autocorrelation. PloS one. 2013; 8(7): e68336.
42. Hu X., Ma C., Huang P., Guo X. Ecological vulnerability assessment based on AHP-PSR method and analysis of its single parameter sensitivity and spatial autocorrelation for ecological protection-A case of Weifang City, China. Ecol. Indic. 2021; 125(1): 107464.
43. Ding L., Chen K.L., Liu T., Cheng S.G., Wang X. Spatial-temporal hotspot pattern analysis of provincial environmental pollution incidents and related regional sustainable management in China in the period 1995-2012. Sustainability 2015; 7(10): 14385-14407.
44. Kumar S., Parida B.R. Hydroponic farming hotspot analysis using the Getis-Ord Gi* statistic and high-resolution satellite data of Majuli Island, India. Remote Sens. Lett. 2021; 12(4): 408-418.
45. Tola A.M., Demissie T.A., Saathoff F., Gebissa A. Severity, spatial pattern, and statistical analysis of road traffic crash hot spots in Ethiopia. Appl. Sci. 2021; 11(19): 8828.
46. Getis A., Ord J.K. The analysis of spatial association by use of distance statistics. Geogr. Anal. 1992; 24(3): 189-206.
47. Shanani H.S., Zarei H. Comparison of Three Classification Algorithms (ANN, SVM, and Maximum Likelihood) for Preparing land-use Map (Case Study: Abolabbas Basin). Iran. J. Water. Manag. Sci. 2015; 10(33): 73-84.
48. Timilsina N., Escobedo F.J., Cropper W.P, Abd-Elrahman A., Brandeis T.J., Delphin S., Lambert S. A framework for identifying Carbon hotspots and forest management drivers. J. Environ. Manag. 2013; 114(1): 293-302.
49. Li G., Wu Z., He Y., Chen C., Long Y. The promotion of sustainable land-use planning for the enhancement of ecosystem service capacity: Based on the FLUS-INVEST-RUSLE-CASA model. Plos one. 2024; 19(7): e0305400.
50. Wang X., Zhang W., Zhao X., Wang D., Li Y. Sustaining Carbon Storage: An Analysis of land-use and Conservation Strategies in China's Huang-Huai-Hai Plain. Sustainability 2024; 17(1): 139.
51. Faraji F., Alijanpour A., Sheidai Karkaj E., Motamedi J. Effect of fire and rangeland banqueting on soil Carbon sequestration in Atbatan summer rangelands, East Azerbaijan Province. ECOPERSIA 2019; 7(1): 29-37.
52. Fan L, Cai T, Wen Q, Han J, Wang S, Wang J, Yin C. Scenario simulation of Land-use change and Carbon storage response in Henan Province, China: 1990-2050. Ecol. Indic. 2023; 154: 110660.
53. Akrofi M.M. Green hotspots? Unveiling global

hotspots and shifting trends in Carbon credit projects. Sustain. Dev. 2025; 33(2): 1782-1796.
54. Hou W., Liu F., Zhang Y., Dong J., Lin S., Wang M. Research Progress and Hotspot Analysis of Low-Carbon Landscapes Based on CiteSpace Analysis. Sustainability 2024; 16(17): 7646.
55. Hwang Y.S., Schlueter S., Pradhan B., Um J.S. Unlocking the potential of ChatGPT in detecting the XCO2 hotspot captured by the Orbiting Carbon Observatory-3 satellite. Sci. Rep. 2025; 15(1):28969.